Experimental Brain Research (2019) 237:1361–1374
https://doi.org/10.1007/s00221-019-05510-5

RESEARCH ARTICLE

Preparation to a quick whole-body action: control with referent body orientation and multi-muscle synergies

Alethéa Gomes Nardini[1,2] · Sandra M. S. F. Freitas[1,3,4] · Ali Falaki[3,5] · Mark L. Latash[3]

Received: 10 December 2018 / Accepted: 7 March 2019 / Published online: 15 March 2019

Abstract

We examined the control of postural stability in preparation to a discrete, quick whole-body sway toward a target and back to the initial position. Several predictions were tested based on the theory of control with referent body orientation and the notion of multi-muscle synergies stabilizing center of pressure (COP) coordinate. Healthy, young adults performed fast, discrete whole-body motion forward-and-back and backward-and-back under visual feedback on the COP. We used two methods to assess COP stability, analysis of inter-trial variance and analysis of motor equivalence in the muscle activation space. Actions were always preceded by COP counter-movements. Backward COP shifts were faster, and the indices of multi-muscle synergies stabilizing COP were higher prior to those actions. Patterns of muscle activation at the motion onset supported the idea of a gradual shift in the referent body orientation. Prior to the backward movements, there was a trend toward higher muscle co-activation, compared to reciprocal activation. We found strong correlations between the sets of indices of motor equivalence and those of inter-trial variance. Overall, the results support the theory of control with referent coordinates and the idea of multi-muscle synergies stabilizing posture by confirming a number of non-trivial predictions based on these concepts. The findings favor using indices of motor equivalence in clinical studies to minimize the number of trials performed by each subject.

Keywords Postural control · Synergy · Variance · Motor equivalence · Referent orientation

Introduction

Two main views dominate the field of motor control. According to one of the views, the central nervous system (CNS) performs computational operations to ensure that proper time profiles of muscle activations and forces are generated by the involved effectors; this is done with the help of internal models or other computational tools such as optimal feedback control schemes (Wolpert et al. 1998; Kawato 1999; Todorov 2004; Shadmehr and Wise 2005; Diedrichsen et al. 2010). The alternative view does not assume neural computation and postulates that the CNS specifies time profiles of parameters of laws of nature that define interactions among body parts and between the body and the environment (Feldman 2015; Latash 2010, 2016, 2017). For example, the dependence of active muscle force on muscle length has features common across skeletal muscles and species; it can be viewed as a biology-specific law of nature that links two salient variables (force and length) with the help of one parameter (threshold of the stretch reflex, λ, as in the equilibrium-point hypothesis, Feldman 1966, 1986). Changes in such parameters are used as tools by the CNS to drive salient performance variables to a desired state.

A generalization of this approach is the theory of motor control with shifting referent coordinates (RCs) for the effectors (reviewed in Feldman 2015). According to this theory, the CNS specifies time profiles of spatial RCs, and the differences between actual coordinates and RCs lead to muscle

✉ Mark L. Latash
mll11@psu.edu

1 Graduate Program in Physical Therapy, City University of São Paulo, São Paulo, SP, Brazil

2 Undergraduate Program in Physical Therapy, University of Paulista, São Paulo, SP, Brazil

3 Department of Kinesiology, Rec.Hall-267, The Pennsylvania State University, University Park, PA 16802, USA

4 Department of Neurology, Milton S. Hershey Medical Center, The Pennsylvania State University, Hershey, PA, USA

5 Département de Neurosciences, Faculté de Médecine, Université de Montréal, Montreal, QC, Canada

activations and active force generation. This process starts at a low-dimensional, task-specific level and then leads to RCs for the involved limbs, joints, and muscles as a result of few-to-many abundant transformations (Latash 2010, 2012). In particular, during standing, referent orientation (RO) of the body is specified at the task level leading to referent joint configurations and RCs for muscles equivalent to their stretch reflex threshold values (λ) as in the classical equilibrium-point hypothesis (Feldman 1966, 1986).

The mentioned few-to-many transformations are typically organized in a synergic way. This means that they allow relatively low stability (reflected in high inter-trial variance) in directions that preserve the task-specific salient variable—these directions span the uncontrolled manifold (UCM, Scholz and Schöner 1999) for that variable—as compared to directions that lead to changes in the salient variable. The UCM concept assumes that the neural controller acts in a multi-dimensional space of elemental variables and stabilizes directions in that space that lead to changes in task-specific salient performance variables. Analysis within the UCM hypothesis involves decomposition of inter-trial variance into a component that keeps a potentially important performance variance unchanged (within the UCM for that variable, V_{UCM}) and a component within the orthogonal to the UCM space (ORT, V_{ORT}), where this variable changes (reviewed in Latash et al. 2002). In our study, elemental variables were associated with muscle groups with parallel scaling of activation levels, muscle modes (*M*-modes, Krishnamoorthy et al. 2003a, b), which are sometimes addressed as "muscle synergies" (Ivanenko et al. 2004; Ting and Mcpherson 2005). We prefer to use the term "synergy" for a neural organization that stabilizes salient performance variables; hence, we address muscle groups with parallel scaling of activation as *M*-modes to avoid confusion.

M-modes have been viewed as reflections of a preferred set of primitives (cf. Bizzi et al. 1995; D'Avella et al. 2003, 2005; Kargo et al. 2010), i.e., RC changes at the joint level, which can be applied with different gains during whole-body tasks (Robert and Latash 2008). The relative amount of inter-trial variance in the *M*-mode space that preserves coordinate of the center of pressure (COP), V_{UCM}, has been used as a metric of postural stability (Danna-dos-Santos et al. 2008; Klous et al. 2011).

The current study aimed to examine several predictions of the theory of postural control with RCs with respect to postural stability in preparation to a quick whole-body sway to a target and back to the initial posture. Imagine a person standing while leaning forward (Fig. 1). To keep balance, referent orientation (RO, a specific example of RC) of the body has to be behind the person (dashed line in Fig. 1) leading to the generation of active moment of force (M_{ACT}) counteracting the moment (M_G) produced by the gravity force. In this posture, elevated background activation of dorsal muscles is

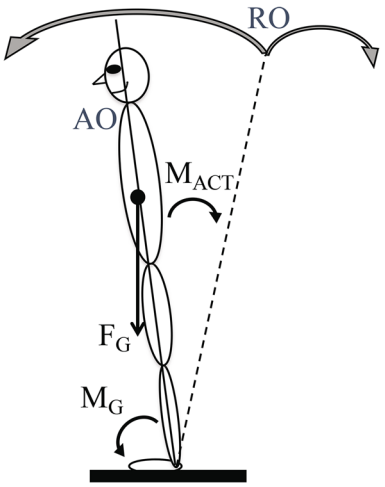

Fig. 1 When a person stands while leaning forward, referent body orientation (RO) differs from the actual body orientation (AO). This leads to the generation of active moment of force (M_{ACT}) counteracting the moment (M_G) produced by the gravity force (F_G). A voluntary body sway is produced by a gradual shift of RO (shown with gray arrows). This scheme leads to several non-trivial predictions (see text)

expected because they are longer compared to their length in the RO, possibly with some co-activation of their antagonists (e.g., Yamagata et al. 2018). To produce a quick sway forward, RO has to be shifted toward the actual body orientation leading, first, to a drop in the dorsal muscle activation (such as in triceps surae, TS) and then, after a delay, to the activation of ventral muscles (such as tibialis anterior, TA). Note that this prediction (our Hypothesis 1) is non-trivial: It predicts that a quick action begins not with the generation of active muscle forces moving the body in the desired direction, but with a drop in the activation of muscles allowing external forces to initiate the desired action (as suggested by Mullick et al. 2018). The prediction is based on assuming a gradual shift in RO, not its jump to the desired final location (cf. Polit and Bizzi 1978; Latash and Gottlieb 1991).

In contrast, motion in the backward direction starting from the same initial posture is expected to begin with a burst of activation of the pre-activated TS. This gives the backward motion an advantage compared to the forward one and is expected to lead to faster sway (Hypothesis 2). The mentioned advantage is due to two factors. One is related to muscle mechanics, which allows expecting larger forces from relatively longer, pre-activated muscles (Zatsiorsky and Prilutsky 2012). The other is due to the fact that, during forward sway, only gravity-related moment is expected to contribute to body motion in the desired direction until RO catches up with the actual body configuration (see Fig. 1). In contrast, during the backward sway, muscle activation contributes to the sway from the very beginning of the RO shift.

Since we allowed the subjects to practice, they could appreciate that backward actions were faster than the

forward ones. This allowed the subjects to prepare for the instructed action differently depending on its direction in spite of the fact that their initial body posture was the same. We expected the subjects to co-activate muscles stronger in preparation to backward sway (Hypothesis 3) because higher muscle co-activation results in higher apparent stiffness of the involved effectors and facilitates faster movement (Bennett et al. 1992; Nielsen and Kagamihara 1992; reviewed in; Latash 2018). Note that changing muscle co-activation without a COP shift (which was prescribed in the initial posture) leads to *M*-mode changes within the UCM for the COP. This is expected to lead to higher V_{UCM} during steady state prior to backward sway (Hypothesis 4) reflecting the signal-dependent noise (Harris and Wolpert 1998).

We also explored a complementary method of quantifying the stability of multi-element states, addressed as analysis of motor equivalence (ME, Mattos et al. 2011, 2013). This method quantifies deviations in a multi-dimensional system of elemental variables (such as *M*-modes) during quick actions in directions that keep a salient performance variable unchanged (within the UCM, motor equivalent, *ME*) and in directions that change that variable (orthogonal to the UCM, non-motor equivalent, *nME*). Assuming that the states of the multi-element system are sampled from the same normal distribution, $\sqrt{V_{UCM}}$ is expected to correlate with *ME*, while the square root from variance in the orthogonal direction, $\sqrt{V_{ORT}}$, is expected to correlate with *nME* (Leone et al. 1961). Indeed, studies of cyclical whole-body sway confirmed strong correlations between the two pairs of indices (Falaki et al. 2017). In contrast, a study of quick multi-finger action (Cuadra et al. 2018) has confirmed only the correlation between $\sqrt{V_{UCM}}$ and *ME*, but not between $\sqrt{V_{ORT}}$ and *nME*. The two mentioned studies differed in the effector (whole body vs. hand), sets of elemental variables (*M*-modes vs. finger modes), and tasks (cyclical sway vs. discrete force pulse). We tentatively expected correlations between both pairs of variables (Hypothesis 5) based on the mentioned study by Falaki et al. (2017).

Methods

Participants

Nine healthy, young subjects, five males and four females, with the age 30.3 ± 3.8 years (mean ± standard deviation, SD), mass 68.1 ± 4.8 kg, and height 1.69 ± 0.06 m participated in this experiment. All participants were right-handed based on their preferential hand usage during writing and eating and had normal or corrected to normal vision. They gave written informed consent according to the procedure approved by the office for research protection of The Pennsylvania State University. The number of participants was defined based on previous studies of multi-muscle synergies during voluntary whole-body tasks performed by healthy, young individuals, which showed moderate-to-large effects of factors such as speed and direction of action (Wang et al. 2006; Danna-Dos-Santos et al. 2008).

Apparatus

The subjects stood barefoot on a force platform (OR-6, AMTI, Watertown, MA, USA) that was used to record three components of the ground reaction force (F_X, F_Y, and F_Z) as well as moments of force (M_X, M_Y and M_Z). The force plate coordinate system was defined with the *X*-axis pointing forward along the AP direction, the *Y*-axis pointing to the right along the ML direction, and the *Z*-axis pointing downward in the vertical direction. These data were used to compute the COP coordinates in the anterior–posterior (COP_{AP}) and medial–lateral (COP_{ML}) directions (cf. Winter et al. 1996). Direct visual feedback on the COP coordinates was presented to the participants with a video projector, which projected on a wall, 2.5 m in front of them at the eye level. Displacements of COP_{AP} caused the cursor to move up and down, while COP_{ML} motion caused cursor motion left and right. Two yellow circles that showed the anterior and posterior targets (see later and Fig. 2) were also displayed on the wall. The normal lights in the laboratory were always on. This did not interfere with the subjects' ability to see the target and feedback on the screen.

The surface electromyograms (EMG) were recorded using a 16-channel Trigno Wireless System (Delsys Inc., Natick, MA, USA). Active electrodes with built-in amplifiers were attached to the skin over the bellies of the following 13 muscles on the right side of the body (Fig. 2): tibialis anterior (TA), soleus (SOL), gastrocnemius medialis (GM), gastrocnemius lateralis (GL), biceps femoris (BF), semitendinosus (ST), rectus femoris (RF), vastus lateralis (VL), vastus medialis (VM), tensor fasciae latae (TFL), lumbar erector spinae (ESL), thoracic erector spinae (EST), and rectus abdominis (RA). EMG sensors were placed according to published guidelines (Criswell and Cram 2011) and subsequently confirmed by observing EMG patterns during isometric contractions and movements. The skin was rubbed with 70% alcohol solution and, when necessary, the leg was shaved before placing the electrodes. The signals from the electrodes were amplified and band-pass filtered (20–450 Hz) before being transmitted to the base station connected to the data collection computer (Dell, Core i7 2.93 GHz). All the signals were sampled at 1000 Hz with a 16-bit resolution analog-to-digital board (PCI 6225, National Instruments Co., Austin, TX, USA). A customized LabVIEW-based software (LabVIEW 2013—National Instruments) was used to record EMG and force platform signals during the experiment.

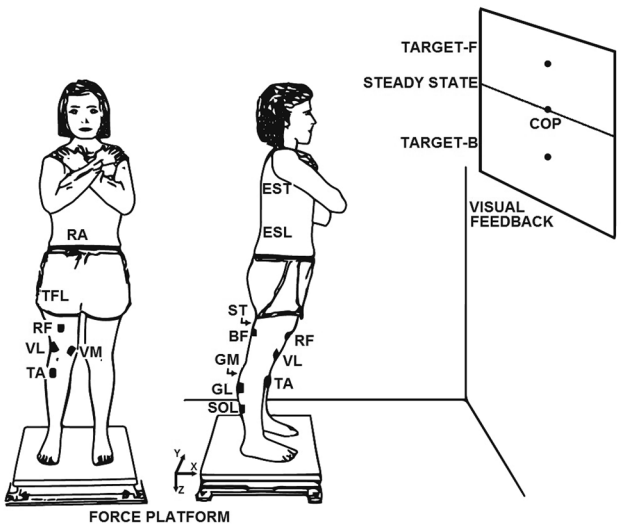

Fig. 2 An illustration of the experimental setup and participant's initial position with the arms across the chest. The black circle on the horizontal line displayed on the screen showed the initial COP position at the steady state. The other two black circles showed the targets for COP shifts forward (Target-F) and backward (Target-B). The electrode placement on the right side of the body is shown with black rectangles except for the rectus abdominis (RA); thoracic erector spinae (EST); tensor fasciae latae (TFL) and lumbar erector spinae (ESL). The other electrodes were positioned at *TA* tibialis anterior, *SOL* soleus, *GM* gastrocnemius medialis, *GL* gastrocnemius lateralis, *BF* biceps femoris, *ST* semitendinosus, *RF* rectus femoris, *VL* vastus lateralis, and *VM* vastus medialis

Procedures

In the initial position, subjects stood on the force platform with their feet in parallel, 15 cm apart. The position of each foot was marked on the top of the platform to make this initial position consistent across all trials and conditions. Each participant performed four tasks: (1) quiet standing (QS); (2) control trials; (3) continuous voluntary body sway task, and (4) discrete COP shift task in the anterior (Forward) or posterior (Backward) direction and back to the initial state.

The QS and control trials were performed to normalize EMG signals. The data from the QS trials were used to correct the EMG signals for the baseline levels. The control trials with holding standard loads were used to normalize the EMG values in the continuous body sway and discrete COP shift tasks. A detailed description of the procedure is given in Danna-Dos-Santos et al. (2007). Briefly, in a single trial of the QS task, subjects stood quietly on the force platform with the arms crossed over the chest and looked at a fixed point on the wall in front of them, while trying to prevent voluntary body movements for 60 s. In the control trials, subjects were asked to hold a horizontal bar by grasping the two circular panels at each side of the bar with both hands, the shoulders flexed at 90° and elbows fully extended. The bar was connected to a pulley system that allowed using the 5 kg load to generate either a downward or an upward force. This posture was held for 10 s with a 1-min rest period between the two trials (one for each force direction). During these trials, the participants were asked to stand still, without leaning forward or backward (visually controlled by the experimenter).

In the continuous voluntary body sway task, the subjects crossed the arms over the chest and performed continuous voluntary full-body sways, mainly moving around the ankle joints, in the anterior–posterior direction. By swaying in this direction, the participants shifted the instantaneous COP_{AP} position projected on the wall between two targets (shown as two horizontal lines). Positions of the targets were set at 2 cm posterior and 8 cm anterior to the neutral standing position (10 cm peak-to-peak amplitude) for all tasks. Participants were asked to keep full contact of both feet with the platform surface during the sway (observed by the experimenter) and to minimize the COP_{ML} deviations. The frequency of the continuous voluntary body sway task was set at 0.5 Hz, paced by an auditory metronome set at 1 Hz (reaching a target at each beep). Three 35-s trials were performed with a 30-s rest period in-between.

The adopted position for the main experimental task (Fig. 2), the discrete COP shift task, was similar to the continuous voluntary body sway task. However, the subjects with the arms crossed over the chest were asked to hold an electrical switch in the right hand that was used to demonstrate when they were ready to start the trial. Before starting the trial, participants shifted their COP_{AP} coordinate 3 cm forward to their natural standing position (shown with a black horizontal line in Fig. 2) and were asked to keep that position stable before pressing the switch. The shifted initial position was selected for two reasons: (1) to have non-zero muscle activation levels during the initial steady state (to enable performing the UCM-based analysis); and (2) to have approximately equal ranges of body motion in the forward and backward directions. This position was considered as initial steady state. After reaching the initial steady state, the participants performed a discrete COP shift toward one of the two directions: anterior (Forward condition) or posterior (Backward condition) and back to the initial posture.

The subjects were instructed to perform discrete whole-body motion to a target as soon as its color changed from yellow to red and return to the initial position "as fast as possible" without losing balance. The target was projected on the wall as a yellow circle (shown and described as "black circles" in Fig. 2) 5 cm higher (Forward) or 5 cm lower (Backward) to the initial steady-state position. Subjects were instructed to keep their feet in full contact with the platform at all times. Each participant performed two blocks of eight trials each, with three COP pulses in each trial. Within a block, all trials were toward the same target, forward or backward. In total, each participant performed 48 pulses, 24

for each direction of COP shift. The order of the two blocks of trials was randomized across participants.

Prior to each block, subjects performed five trials (15 pulses) to get familiar with the procedure. Rest intervals of 30 s between trials and 5 min between blocks were given. Additional rest periods were provided if requested. None of the subjects reported fatigue. The whole experimental session lasted for about 50 min.

Data analysis

All signals were processed off-line using a customized Matlab R2016a program (Mathworks Inc, MA, USA). Prior to computing time-varying COP_{AP} coordinates (Winter et al. 1996), data from the force platform were filtered with a 10-Hz low-pass, fourth-order, zero-lag Butterworth filter.

For each trial of the continuous voluntary body sway task, to avoid edge effects and incomplete cycles at the beginning and end of each trial, only the data within {3 s; 30 s} time interval were accepted. The time interval between two consecutive anterior-most COP_{AP} coordinates was defined as a sway cycle. On average, each subject performed 15 cycles within each trial.

Raw EMG data were shifted 50 ms backward with respect to the force platform data to compensate for the electromechanical delay (Corcos et al. 1992), band-pass filtered (20–350 Hz) with a fourth-order, zero-lag Butterworth filter, and then fully rectified. For each subject, filtered EMG of each muscle was corrected for the background activity by removing the baseline muscle activity during the QS trial (EMG_{QS}) defined as the average value within the time interval {13 s; 17 s}. Further, EMGs were normalized by the peak value (EMG_{PEAK}) for each muscle across control trials and continuous voluntary body sway task (Klous et al. 2011):

$$EMG_{NORM} = \frac{EMG - EMG_{QS}}{EMG_{PEAK}}$$

Defining muscle modes

Groups of muscles with parallel scaling of activation levels were defined as muscle modes (*M*-modes). This procedure reduced the 13-dimensional muscle activation space to a three-dimensional *M*-modes space. For this purpose, EMG_{NORM} signals from the continuous voluntary body sway task were integrated over 50-ms time windows ($\int EMG_{NORM}$). For each subject, the $\int EMG_{NORM}$ data from the continuous voluntary body sway task were concatenated to create a matrix with 13 columns representing 13 muscles and the number of rows corresponding to the number of samples across the sway cycles analyzed. Principal component analysis (PCA) with Varimax rotation and factor extraction was applied to the correlation matrix of $\int EMG_{NORM}$ data (Krishnamoorthy et al. 2003a, b; Danna dos Santos et al. 2007). For each subject, the first three principal components (PCs) were selected based on the Kaiser criterion (Kaiser 1960), and each PC had to contain at least one muscle with a significantly high loading (with the absolute magnitude over 0.5; Hair et al. 1995). This procedure produced an orthogonal set of eigenvectors in the muscle activation space, which were multiplied by the rectified EMG data in each time sample of the discrete COP shift trials to define the *M*-mode magnitudes. For each COP shift, t_0 was defined as the instant of time when the COP shift reached 1% of its peak velocity after moving from the initial position. Regardless of movement direction, t_0 was close to the maximum counter-movement of the discrete COP shift (see Fig. 3 in Results). The amplitude of the COP shift and its peak rate were calculated in two phases: during the counter-movement and during the instructed COP shift.

The *M*-modes were used as the elemental variables for further variance and motor equivalence analysis the discrete COP shift task. The *M*-mode data for the first two *M*-modes were used to compute the reciprocal and co-activation indices, *R*-index and *C*-index, respectively (Slijper and Latash 2000, 2004). For this analysis, the *M*-modes were integrated over a 1-s interval starting 1500 ms before the onset of the COP shift (t_0). One of the first *M*-modes united significantly loaded dorsal muscles, whereas the other *M*-mode united significantly loaded ventral muscles (see Results). The *R*-index and *C*-index were defined as:

$$R\text{ - index} = \int(M1 - \text{mode}) - \int(M2 - \text{mode})$$

$$C - \text{index} = 0, \text{ if the two integrated}$$

$$M - \text{mode indices had different signs;}$$

$$C\text{ - index} = \min[|\int(M1 - \text{mode})|, |\int(M2 - \text{mode})|],$$

if the first two integrated *M*-modes had the same sign.

The values of *R*- and *C*-index were normalized by the maximum value obtained across trials and conditions for each subject separately.

Defining the Jacobian matrix

Linear relations between small changes in the magnitude of *M*-modes ($\mathbf{\Delta M}$) and the COP_{AP} shifts (ΔCOP_{AP}) were assumed (Danna-dos-Santos et al. 2007; Krishnamoorthy et al. 2003b). $\mathbf{\Delta M}$ and ΔCOP_{AP} data from the continuous voluntary body sway task were computed within 50-ms time windows. Both $\mathbf{\Delta M}$ and ΔCOP_{AP} were filtered with a 5-Hz, low-pass, fourth-order, zero-lag Butterworth filter (Falaki et al. 2014, 2016). Multiple regression analysis was performed for each subject separately:

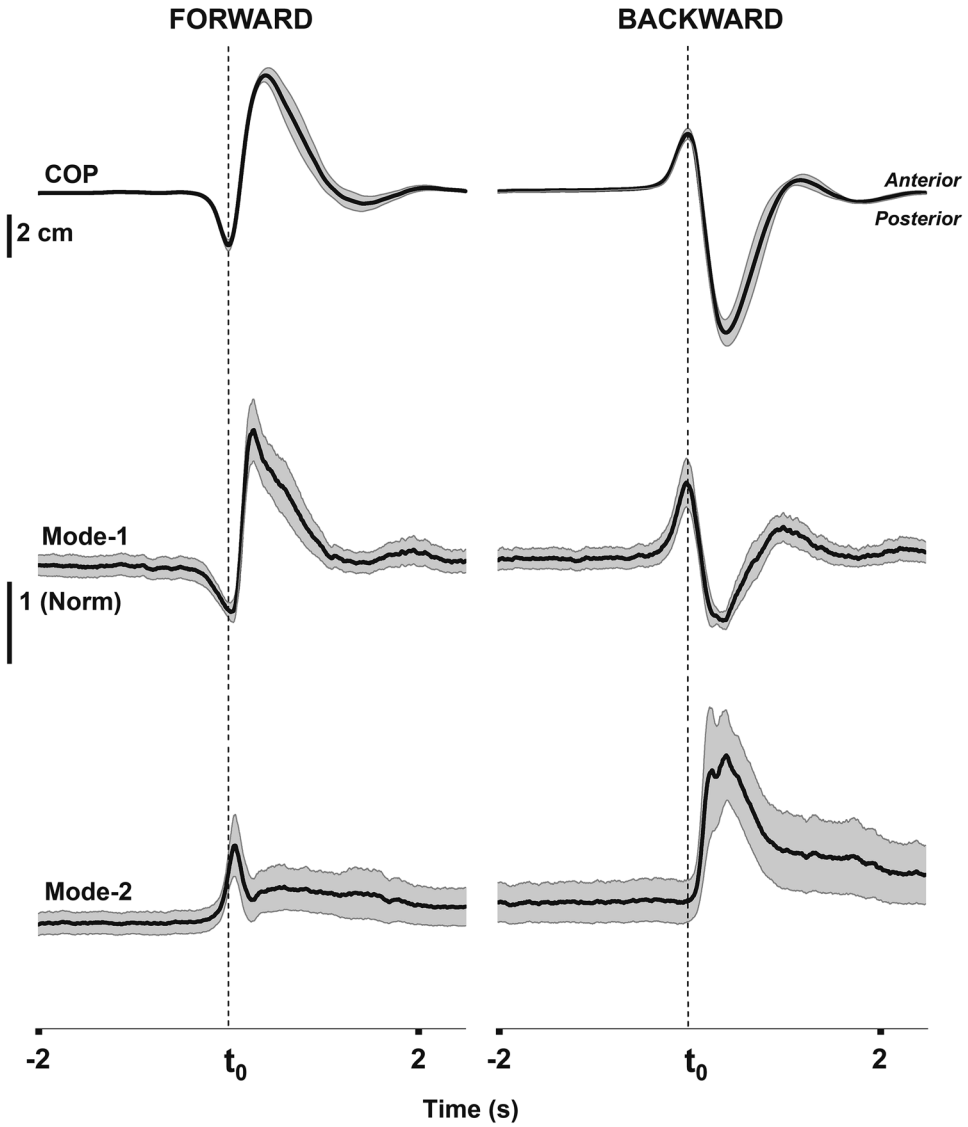

Fig. 3 Averaged across subjects COP trajectories (top panels) and time profiles of the *M1*-mode and *M2*-mode with standard error shades (gray) are shown for the Forward (left) and Backward (right) conditions. *M*-modes are in normalized units

$$\Delta \mathrm{COP}_{\mathrm{AP}} = k_1 \Delta M_1 + k_2 \Delta M_2 + k_3 \Delta M_3$$

where k_{1-3} are constants. The resulting set of coefficients from the regression was arranged in a matrix that is the **J** matrix: $\mathbf{J} = [k_1\ k_2\ k_3]$ for each subject.

Analysis of variance

The framework of the uncontrolled manifold (UCM) hypothesis (Scholz and Schöner 1999) was used to perform two types of analysis, those of inter-trial variance and of motor equivalence. Both analyses were performed within the space of elemental variables associated in our study with *M*-modes. Within the former analysis, inter-trial variance components were quantified within two sub-spaces, the UCM (V_{UCM}, variance preserving the $\mathrm{COP}_{\mathrm{AP}}$ coordinate) and the orthogonal to the UCM space (V_{ORT}, variance affecting the $\mathrm{COP}_{\mathrm{AP}}$ coordinate). The *M*-mode space had the dimensionality of $n = 3$. Since the hypothesis of $\mathrm{COP}_{\mathrm{AP}}$ stabilization accounted for 1 degree of freedom ($d = 1$), the UCM was two-dimensional.

For each participant, the residual mean-free vectors of *M*-modes ($\mathbf{\Delta M}_{\mathrm{demeaned}}$) were calculated by subtracting the mean magnitude of the *M*-modes across trials ($\overline{\Delta \mathbf{M}}$) from the changes in the *M*-mode magnitudes ($\mathbf{\Delta M}$):

$$\Delta \mathbf{M}_{\mathrm{demeaned}} = \Delta \mathbf{M} - \overline{\Delta \mathbf{M}}$$

V_{UCM} and V_{ORT} during the steady-state phase (the time interval from 1500 ms to 500 ms before t_0) across pulses per degree of freedom of the respective space were calculated as:

$$V_{\mathrm{UCM}} = \sigma^2_{UCM} = \sum_{I=1}^{N} f^2_{\mathrm{UCM}} / (n-d) N_{\mathrm{trials}}$$

$$V_{ORT} = \sigma^2_{ORT} = \sum_{I=1}^{N} f^2_{ORT} / (dN_{trials})$$

where f_{UCM} and f_{ORT} represent the projection of the mean-free $\Delta\mathbf{M}$ onto the UCM and ORT.

Analysis of motor equivalence

The motor equivalence analysis (Mattos et al. 2011, 2013) quantified the amount of deviation between the two steady-state intervals (before and after each COP_{AP} pulse) in the space of elemental variables (*M*-modes) in directions preserving (motor equivalent, *ME*) or changing (non-motor equivalent, *nME*) COP_{AP}. This analysis was performed within each trial for each COP_{AP} pulse separately. For each pulse, deviations of *M*-modes from the initial steady state to the one following the COP_{AP} shift were projected onto the null-space of $\boldsymbol{J}$ and on its orthogonal complement. The two steady-state intervals were defined as 500-ms intervals ending 500 ms prior to t_0 and starting 2000 ms after t_0. These intervals were defined based on two factors: (1) to avoid including any anticipatory preparation to the action, which we expected to start not earlier than 500 ms prior to t_0 based on earlier studies (Klous et al. 2011); and (2) to give the subject sufficient time to return to the initial position (based on the pilot data, we estimated this time as 1.5 s). The length of this projection within the UCM was the *ME* component, whereas the length of the projection within the ORT space was the *nME* component. *ME* and *nME* indices were normalized per square root of the dimension of the corresponding space (cf. Falaki et al. 2017). Averaged across pulses *ME* and *nME* were computed for each subject and each condition.

Statistics

Statistical analysis was performed with SPSS 20 (IBM Corp., Armonk, NY, USA). The normality of the data distribution was checked before further statistical analysis with the Shapiro–Wilk test. In cases of violation of the normality assumption, data were log-transformed before parametric analysis. Data are presented in the text, tables, and figures as means and standard errors. The coefficients of determination (R^2) are presented as median and interquartile range (IQR) values. Two-way, repeated measures (RM) analysis of variance (ANOVA) with factors phase (counter-movement vs. COP shift toward the target) and Condition (Forward vs. Backward) were run for comparisons of the amplitude of the COP shift and the peak rate of COP displacements (*dCOP*/*dt*). A two-way, RM-ANOVA with factors Condition and Mode (*M*1-mode vs. *M*2-mode) was run to compare the magnitude of the first two *M*-modes. These analyses were run to investigate Hypotheses 1 and 2. To test Hypothesis-3, RM-ANOVA with factors Condition and Index (*R*-index vs. *C*-index) was performed on reciprocal and coactivation indices.

Two RM-ANOVAs with factors Condition and Component (*UCM* vs. *ORT* and *ME* vs. *nME*, depending on the analysis) were run to test the fourth Hypothesis. To test the fifth Hypothesis, Pearson correlation coefficients were computed to explore the relationship between the indices of inter-trial variance and motor equivalence. For all statistical analyses, we assume $\alpha = 0.05$.

Results

General patterns of mechanical and EMG variables

All participants always started a voluntary quick COP_{AP} shift with a small-amplitude deviation from the initial COP position in the opposite direction, i.e., away from the prescribed target. That is, forward COP_{AP} shifts were initiated by COP displacements in the posterior direction while backward COP_{AP} shifts were initiated by moving the COP forward. This counter-movement of the COP can be seen in Fig. 3 in the COP_{AP} displacement time series averaged across all pulses and participants.

Based on the continuous voluntary body sway task, three *M*-modes were identified with the PCA with rotation and factor extraction on the $\int EMG_{NORM}$ indices. Averaged across the subjects muscle loadings for each *M*-mode and the amounts of explained variance accounted by the PCs are presented in Table 1. The total amount of explained variance was, on average, $74.6 \pm 1.7\%$. The first two *M*-modes showed consistent loading patterns of individual muscle activation indices, while *M*3-mode was much more variable across subjects.

The time profiles of the first two *M*-modes, *M*1-mode and *M*2-mode, during the voluntary COP pulse are also illustrated in Fig. 3. The *M*1-mode contained significantly loaded dorsal muscles, including the ankle extensors (plantar flexors), while the *M*2-mode contained significantly loaded ventral muscles (including TA). For the forward target (left panels), the *M*1-mode showed a drop (reaching its minimum close to t_0) followed by a *M*2-mode activation burst and, later, a delayed activation burst of the *M*1-mode. For the backward target (right panels), the COP motion started with an activation burst of the *M*1-mode followed by a delayed burst of the *M*2-mode and a delayed small second burst in the *M*1-mode. These patterns were similar across participants.

Table 1 Muscle loadings for the three *M*-modes

Explained variance (%)	*M*1 37.7 ± 5.9	*M*2 24.4 ± 5.3	*M*3 12.6 ± 5.7
TA	−0.38 ± 0.13	**0.56 ± 0.09**	−0.09 ± 0.06
SOL	**0.74 ± 0.08**	−0.25 ± 0.07	0.18 ± 0.11
GM	**0.80 ± 0.03**	−0.34 ± 0.04	0.13 ± 0.06
GL	**0.80 ± 0.04**	−0.27 ± 0.02	0.13 ± 0.08
BF	**0.72 ± 0.11**	−0.06 ± 0.12	0.14 ± 0.06
ST	**0.86 ± 0.01**	−0.20 ± 0.03	0.14 ± 0.06
RF	−0.27 ± 0.05	**0.77 ± 0.03**	0.00 ± 0.04
VL	−0.29 ± 0.05	**0.81 ± 0.02**	0.01 ± 0.04
VM	−0.19 ± 0.05	**0.83 ± 0.02**	−0.01 ± 0.02
TFL	0.08 ± 0.13	**0.49 ± 0.14**	0.06 ± 0.10
ESL	**0.62 ± 0.09**	−0.20 ± 0.06	0.30 ± 0.10
EST	**0.54 ± 0.10**	−0.18 ± 0.06	0.35 ± 0.12
RA	0.06 ± 0.05	0.12 ± 0.08	**0.70 ± 0.14**

Averaged across-subjects values are presented ± standard error. Significant loading factors are shown in bold and highlighted

TA tibialis anterior, *SOL* soleus, *GM* gastrocnemius medialis, *GL* gastrocnemius lateralis, *BF* biceps femoris, *ST* semitendinosus,*RF* rectus femoris, *VL* vastus lateralis, *VM*: vastus medialis, *TFL* tensor fasciae latae; *ESL* lumbar erector spinae, *EST* thoracic erector spinae, *RA* rectus abdominis

COP trajectories

The amplitude of the initial COP shift away from the target did not differ between the two conditions (on average 3.2 cm, see Table 2), while the COP shift toward the target was larger for the backward target location (Table 2). This was confirmed by a significant *Phase* × *Direction* interaction ($F_{1,8} = 6.58$; $p < 0.05$; $\eta_p^2 = 0.45$). The absolute peak rate of COP shift was significantly higher for the posterior target compared to the anterior target (by about 20%) without a significant difference between these values for the initial COP deviation away from the target (Table 2; *Phase* × *Direction* interaction, $F_{1,8} = 14.6$; $p < 0.01$; $\eta_p^2 = 0.67$).

During the initial steady-state phase, the magnitude of the *M*1-mode was similar to that of the *M*2-mode prior to the backward COP shift, whereas the *M*1-mode magnitude was greater than that of the *M*2-mode for the forward COP shift (Fig. 4a). These findings were confirmed by the significant *Mode* × *Condition* interaction ($F_{1,8} = 5.35$; $p = 0.05$; $\eta_p^2 = 0.4$).

To examine whether there was stronger muscle co-activation in preparation to COP shifts towards the backward target compared to the forward target, we compared the indices of reciprocal activation and co-activation between the *M*1-mode and *M*2-mode (*R*-index and *C*-index, Fig. 4b) between the two conditions. ANOVA showed no significant main effects, but there was a significant interaction *Index* × *Condition* ($F_{1,8} = 9.11$; $p < 0.05$; $\eta_p^2 = 0.53$). In particular, the *R*-index was significantly greater for the Forward compared to the Backward condition, while the *C*-index was larger for the Backward condition, although this difference was below the level of significance (Fig. 4b).

Table 2 COP characteristics

	Forward		Backward	
COP amplitude (cm)				
Initial, away from the target	3.1	±0.2	3.3	±0.2
Toward the target	9.5	±0.6	11.1	±0.8
Median (IQR)				
Initial, away from the target	3.3	(1.25)	3.4	(1.0)
Toward the target	8.6	(3.11)	10.4	(3.6)
$[dCOP/dt]_{MAX}$ (cm/s)				
Initial, away from the target	19.01	±2.6	15.2	±1.5
Toward the target	51.5	±4.3	69.8	±7.4
Median (IQR)				
Initial, away from the target	20.7	(13.8)	16.7	(6.8)
Toward the target	49.8	(20.6)	61.4	(44.9)

$[dCOP/dt]_{MAX}$ represents the absolute value of the peak rate of COP shift

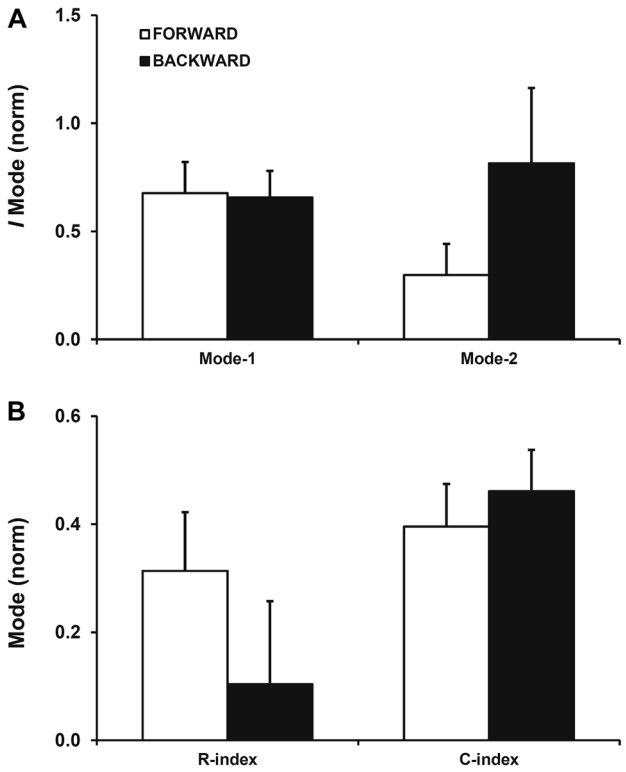

Fig. 4 Across-subject means and standard errors for the *M*-modes magnitude (**a**) and reciprocal and coactivation (respectively, *R*- and *C*-) indices (**b**) computed over the steady state for the Forward (white bars) and Backward (black bars) conditions

M-mode variance and motor equivalence analyses

We used multiple linear regression to link small changes in *M*-modes to COP_{AP} shifts. This analysis confirmed that each *M*-mode was a significant predictor of COP_{AP} shifts. The adjusted median R^2 value was 0.76 (IQR = 0.71–0.80).

Analysis of the inter-trial variance in the *M*-mode space within the framework of the UCM hypothesis (see "Methods" section) showed significantly larger values of the *M*-mode variance within the UCM compared to variance in the orthogonal direction, $V_{UCM} > V_{ORT}$ (Fig. 5a). This difference was confirmed by a significant effect of *Component* ($F_{1,8} = 6.74$; $p < 0.05$; $\eta_p^2 = 0.46$). There was also a significant *Condition* × *Component* interaction ($F_{1,8} = 16.78$; $p < 0.01$; $\eta_p^2 = 0.68$) reflecting the larger difference between V_{UCM} and V_{ORT} for the Backward condition.

Analysis of motor equivalence confirmed significantly large *ME* deviations compared to *nME* deviations (Fig. 5b, $F_{1,8} = 6.08$; $p < 0.05$; $\eta_p^2 = 0.43$) between the two steady states, prior to the COP shift and after the shift. There were no significant differences between the Backward and Forward conditions.

The relationships between $\sqrt{V_{UCM}}$ and *ME* and between $\sqrt{V_{ORT}}$ and *nME* were explored using Pearson correlation coefficients for each condition (Forward and Backward; Fig. 6). The correlations for both pairs of variables were significant for both directions of COP_{AP} shift.

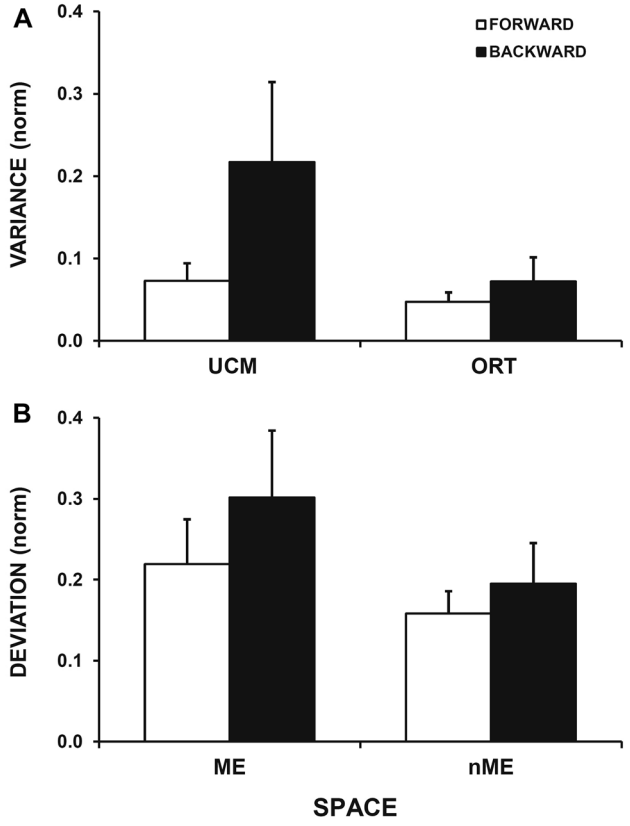

Fig. 5 **a** The inter-trial variance components computed within the UCM space and orthogonal to it (ORT), normalized per dimension, computed over the steady state before the discrete COP shift for the Forward (white bars) and Backward (black bars) conditions. **b** The indices of motor equivalence (*ME* and *nME*) analysis for the Forward and Backward conditions (respectively, white and black bars) computed between the initial steady state and final steady state. Averaged across subjects values are shown with standard error bars

Discussion

The results confirmed most of the predictions drawn in the "Introduction" based on two theoretical concepts. The first is the theory of control of posture and movement with shifts in referent coordinates for effectors (reviewed in Latash 2010; Feldman 2015); according to this theory, the control of whole-body movements can be adequately described with changes in referent body orientation (RO; see Mullick et al. 2018). The second is the idea of synergic control of multi-muscle systems stabilizing salient performance variables (reviewed in Latash et al. 2007).

As predicted by Hypothesis 1, forward body sway started with a drop in the *M*1-mode (with dorsal muscles

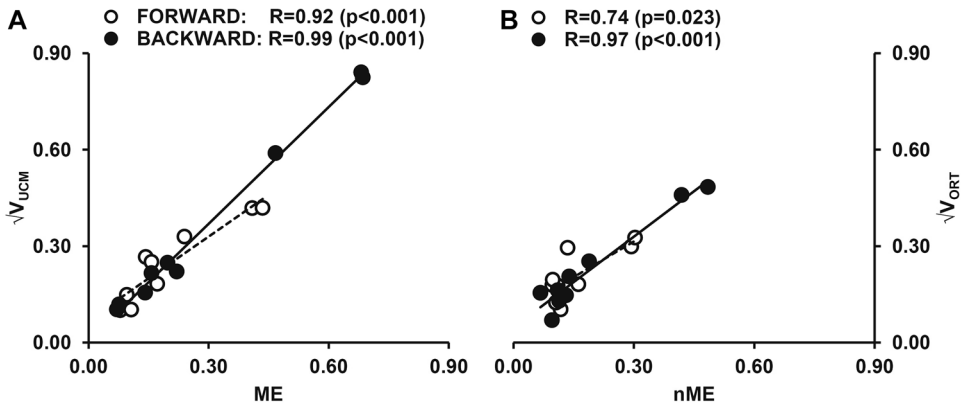

Fig. 6 Scatter plots showing the relationship between $\sqrt{V_{UCM}}$ and *ME* (**a**) and $\sqrt{V_{ORT}}$ and *nME* (**b**) calculated for the same time intervals as in Fig. 5. The data for the Forward (white circles) and Backward (black circles) conditions are shown. The Pearson correlation coefficients are presented

significantly loaded) magnitude followed by an increase in the *M*2-mode activation (reflecting, in particular, a commonly seen EMG burst in the tibialis anterior). In contrast, the backward sway started with an activation burst in the *M*1-mode and was associated with faster peak COP speed as predicted by Hypothesis 2. The subjects showed higher index of reciprocal activation (*R*-index) prior to the forward sway, whereas the co-activation index (*C*-index) tended to be higher prior to the backward sway (cf. Hypothesis 3). The preparation to the backward sway was associated with a significantly higher inter-trial variance in the *M*-mode space that had no effect on the COP coordinate (V_{UCM}, Hypothesis 4). Hypothesis 5 predicted correlation between $\sqrt{V_{ORT}}$ and *nME* and between, $\sqrt{V_{UCM}}$ and *ME* indices. This hypothesis has been confirmed for both directions of postural sway.

Control of posture and movement with referent coordinates

At the level of control of single muscles, the idea of control with spatial referent coordinates associates parameters manipulated by the CNS with subthreshold depolarization of respective alpha-motoneuronal pools, equivalent to magnitude of the stretch reflex threshold (Feldman 1986). For multi-muscle systems, including whole-body actions, the idea has been generalized assuming that the parameter modified by the CNS represents spatial RCs for the effectors. For example, during natural standing, the body center of mass typically projects in front of the ankle joints and generates a moment of force in a sagittal plane. This moment is counteracted by an active moment of force generated by the RO of the body being slightly behind its actual orientation (cf. Mullick et al. 2018). If the person is asked to lean forward, as in our experiment, the difference between the RO and actual body orientation is expected to increase (illustrated in Fig. 1 in the Introduction). Assuming that the person leans forward primarily by moving the ankle joints (as instructed in our study), the ankle extensors (TS) are expected to show elevated activation level during quiet standing in this posture.

If the CNS programmed forces and/or muscle activations, a quick forward sway would be expected to start with a burst of TA activation, with or without a drop in the TS activity. Indeed, higher co-activation is useful for fast actions because it increases the apparent stiffness of the joints (Frysinger et al. 1984; Hirokawa et al. 1991). The idea of control with RO makes a different prediction. The action is initiated by a shift of RO forward leading to a drop in the TS activation level and, only after a delay, to a burst in TA. We observed the latter pattern in all subjects (illustrated in the *M*-mode space in Fig. 3) in support of the idea of control with RO. This pattern is similar to the one reported by Mullick et al. (2018) in their study of standing on inclined surfaces.

The asymmetry of RO with respect to the actual body orientation also predicts an asymmetry in EMG patterns associated with quick sway in the forward and backward directions. This was indeed observed in our study. While backward sway was initiated by an EMG burst in the agonist group (TS), as would also be expected from the schemes of control with muscle activation patterns (cf. Gottlieb et al. 1989), forward sway was initiated by a drop in the background EMG, which is expected from the control with RO but not from EMG-control schemes.

A consistent pattern of COP shifts included a transient motion in the direction away from the target (see Fig. 2). Such patterns were described in earlier studies prior to quick intentional changes in the COP coordinate (Wang et al. 2006). The early COP shift is a mechanical necessity to produce a moment of force rotating the body in the desired direction. As such, it belongs to the class of so-called early postural adjustments (EPAs, Krishnan et al. 2011) similar to those observed prior to step initiation (Breniere and Do 1986; Crenna and Frigo 1991; see the next section).

Control of stability in preparation to action

Preparation to a quick action from steady state is associated with a number of anticipatory (feed-forward) phenomena. These include the well-known anticipatory postural adjustments (APA, Belenkiy et al. 1967; Massion 1992) seen as changes in the background muscle activation prior to a quick action or a predictable perturbation. APAs are seen about 100 ms prior to action/perturbation initiation, they are associated with predictable or self-triggered perturbations and typically produce forces and moments of force to counteract the predicted mechanical effects of the perturbation. Some actions require mechanical adjustments for a planned action to be possible in the absence of perturbations. Such adjustments (EPAs) are typically seen well before the aforementioned APAs, e.g., starting about 0.5 s prior to action initiation. Although postural preparations to action (e.g., to stepping) are commonly addressed as APAs, we think that there are major differences in the function, timing, and control of the two groups of postural adjustments and, therefore, prefer to use different terms, APAs and EPAs (Krishnan et al. 2012). In our study, EPAs have been observed as transient COP deviations away from the target.

Some of our findings, in particular the COP shifts and EMG patterns, resemble those observed prior to gait initiation (Breniere and Do 1986; Crenna and Frigo 1991; Wang et al. 2005). We would like to emphasize, however, a few major differences between our study and those of gait initiation. First, gait initiation leads to transfer of the whole body in space, whereas our task required the subjects to end each trial in a state similar to the initial state. Using the language of referent body coordinates, our task required a transient

change in the referent body orientation only, whereas step initiation requires a change in the referent body coordinate in the external 3D space in addition to transient changes in referent orientation. Note that a change in the body location in space complicates or even makes it impossible to analyze motor equivalence, which was done in our study. Second, gait initiation requires COP shift in the medio-lateral direction to unload the stepping leg, whereas in our study only COP shift in the anterior-posterior direction were required. Third, in contrast to our study, body sway and associated COP shifts are not part of the task in gait initiation.

Recently, another group of anticipatory adjustments to action has been described (Olafsdottir et al. 2005; Shim et al. 2005; Klous et al. 2011; Krishnan et al. 2011; Piscitelli et al. 2017). These phenomena, referred to as anticipatory synergy adjustments (ASAs), are not accompanied by consistent changes in salient performance variables. Instead, they represent changes in stability of those variables, which is typically high during steady state. In young healthy persons, a drop in the stability index is seen about 300 ± 100 ms prior to action initiation. Its purpose is to facilitate future change in the salient variable by making it less stable. ASAs have shown high sensitivity to instruction (Olafsdottir et al. 2005), healthy aging (Olafsdottir et al. 2007), a range of neurological disorders (reviewed in Latash and Huang 2015), and therapy with drugs (Park et al. 2014) and with deep brain stimulation (Falaki et al. 2018).

Tilman and Ambike (2018) have recently described another example of ASAs representing a drop in the stability index when subjects knew that a quick action might be needed, even when no signal for such an action arrived. In our experiment, we observed significantly higher relative amounts of variance within the UCM (V_{UCM}, a metric of postural stability) when the subjects planned a quick sway backward compared to the quick sway forward (note the large V_{UCM} compared to V_{ORT} in Fig. 5A). Since backward sway was associated with faster peak COP speed, this finding looks controversial and conflicting with the cited results of Tilman and Ambike (2018). Indeed, a quicker action is expected to require stronger destabilization of the salient variable (cf. Shim et al. 2005); hence, smaller V_{UCM} could be expected prior to the backward sway actions.

It is well known that the limits of stability measured by the COP excursion in the anterior–posterior direction are asymmetrical with respect to the neutral standing posture (with 2/3 of the range in the anterior direction, Duarte and Freitas 2005). As a result, individuals are expected to feel more confident leaning forward than backward (Rand et al. 2012; Halfström et al. 2014). In the current study, subjects started with the COP moved forward by 3 cm to compensate for the COP range inequality (and also to ensure non-zero muscle activation levels, which are needed for the UCM-based analysis). This adjustment could give them more confidence in moving backward, which could lead to the faster peak COP speed.

There is, however, another factor that might affect the V_{UCM} index. In preparation to quick sway backward, the subjects had a tendency of showing higher values of background muscle activation (Figs. 3, 4a). Since the COP was always at the same location, this could only result from higher muscle co-activation. This strategy sounds reasonable because higher co-activation corresponds to higher apparent stiffness of the effectors, which facilitates quick movements (Corcos et al. 1989; Bennett et al. 1992; Milner and Cloutier 1993). Note also that, by definition, changes in muscle activation that lead to no COP displacements are within the UCM for COP coordinate. So, higher muscle co-activation (accompanied by its higher variance due to the signal-dependent noise, Harris and Wolpert 1998) is expected to lead to disproportionally higher V_{UCM}, which was indeed observed in our study (Fig. 5).

Thus, control of the stability of salient performance variables in preparation to action is a complex phenomenon involving several components. While ASAs seen immediately prior to action initiation are always associated with a drop in the stability of the salient variable (at least, we are unaware of exceptions from this rule), adjustments of stability during steady states may be in different directions. The unexpected increase in V_{UCM} in preparation to the backward sway might be due to the specificity of the task; we have to explore whether similar phenomena can be observed in other effector sets and tasks (such as multi-joint and multi-finger actions).

Metrics of stability in abundant systems

Stability of a variable produced by an abundant set of elemental variables may be seen as stabilization of a subspace in the high-dimensional space of elemental variables (cf. Akulin et al. 2018). This sub-space is orthogonal to the UCM for the salient variable; we have referred to this sub-space as ORT. Several metrics have been developed to explore stability within ORT and UCM. The most commonly used method compares inter-trial variance within UCM and ORT. It is based on the natural notion of trajectories converging along dynamically stable directions (and leading to small variance) and diverging along unstable directions (leading to higher variance). This method has been applied in numerous studies including those of special populations with impaired motor coordination (reviewed in Latash et al. 2007; Latash 2008; Latash and Huang 2015).

Another method has been introduced relatively recently (Scholz et al. 2007; Mattos et al. 2011, 2013). It is based on the idea that a quick action imposed on a multi-element system induces motion of this system primarily along unstable directions, rather than along the desired directions. For

example, if you try to compress quickly a spring (e.g., a typical spring from the pen) held between the index finger and the thumb, the spring will buckle and jump sideways (cf. Venkadesan et al. 2007). This is due to its lower stability in directions orthogonal to its main axis as compared to stability along the main axis. This general idea has resulted in two indices of deviation of the system during quick actions, along the UCM (motor equivalent, *ME*) and along ORT (non-motor equivalent, *nME*).

The two sets of indices, $\{V_{UCM}; V_{ORT}\}$ and {*ME; nME*} are not redundant. Some studies, including the current study, have shown significant correlations between $\sqrt{V_{UCM}}$ and *ME* as well as between $\sqrt{V_{ORT}}$ and *nME* (Falaki et al. 2017; de Freitas et al. 2018) expected from statistical considerations of folded distributions (Leone et al. 1961). These considerations, however, are applicable only if the initial and final values used in the computation of *ME* and *nME* are taken from the same normal distribution, which does not have to be true. For example, a recent study of multi-finger force pulse production (Cuadra et al. 2018) has shown strong correlations between $\sqrt{V_{UCM}}$ and *ME* in the absence of such correlations between $\sqrt{V_{ORT}}$ and *nME*. These findings were interpreted as resulting from corrections introduced by the subjects in the ORT direction but not in the UCM direction, because the visual feedback showed them changes in total force affected only by ORT movements in the finger force space.

One of the differences between the cited studies is that some of them involved cyclical actions while others involved discrete actions. Since potential differences between these two classes have been emphasized recently (Hogan and Sternad 2007), we used in the current study a discrete action (as in Cuadra et al. 2018) in otherwise similar procedure to that of Falaki et al. (2017). Our observations confirmed those made by Falaki et al. (2017) showing significant correlations between both pairs of variables $\sqrt{V_{UCM}}$ vs. *ME* and $\sqrt{V_{ORT}}$ vs. *nME* (Fig. 6). Hence, we conclude that the cyclic–discrete dichotomy was not crucial for these correlations. This finding may be viewed as important for clinical studies as analysis of motor equivalence requires relatively few trials as compared to analysis of inter-trial variance (Freitas et al. 2019). Given that indices of motor equivalence show good-to-excellent reliability (de Freitas et al. 2018), they are attractive indices for changes in action stability in neurological patients (reviewed in Latash and Huang 2015). Note that analyses of both inter-trial variance and motor equivalence in the muscle activation space have shown changes in the synergy indices in PD individuals, even in those without clinical signs of postural instability (Falaki et al. 2017).

Concluding comments

The results of the current study have supported our hypotheses based on the concepts of the control of whole-body movements with changes in body RO and of the multi-muscle synergies stabilizing COP shifts. Some of the observations raised new issues, which need further research to be clarified. One of them is the counter-intuitive higher magnitudes of variance in the *M*-mode space compatible with unchanged COP coordinate (V_{UCM}) prior to the faster COP shift backwards. Based on a recent study (Tillman and Ambike 2018), we could expect an opposite effect. Another counter-intuitive observation is the faster COP shifts backwards. Indeed, humans typically feel less confident shifting COP backwards across a variety of tasks (Rand et al. 2012; Halfström et al. 2014), possibly to minimize chances of backward fall and due to asymmetrical effects of visual information. A more complete study would use two initial body postures with COP shifted both forward and backward with respect to its natural coordinate. We would also like to admit that some effects should be viewed as pilot because they did not reach the level of statistical significance, in particular the differences in the co-activation index prior to the voluntary sway in different directions. These effects require confirmation in a better powered study.

Acknowledgements The study was supported in part by an NIH grant NS082151. This study was financed in part by the Coordenação de Aperfeiçoamento de Pessoal de Nível Superior—Brasil (CAPES) to Nardini—Finance Code 001. Freitas is grateful to CNPq/Brazil.

References

Akulin VM, Carlier F, Solnik S, Latash ML (2018) Sloppy, but acceptable, control of biological movement: Algorithm-based stabilization of subspaces in abundant spaces. J Hum Kinet. https://doi.org/10.2478/hukin-2018-0086

Belenkiy VY, Gurfinkel VS, Pal'tsev YI (1967) Elements of control of voluntary movements. Biofizika 10:135–141

Bennett DJ, Hollerbach JM, Xu Y, Hunter IW (1992) Time-varying stiffness of human elbow joint during cyclic voluntary movement. Exp Brain Res 88:433–442

Bizzi E, Giszter SF, Loeb E, Mussa-Ivaldi FA, Saltiel P (1995) Modular organization of motor behavior in the frog's spinal cord. Trends Neurosci 18:442–446

Breniere Y, Do MC (1986) When and how does steady state gait movement induced from upright posture begin? J Biomech 19:1035–1040

Corcos DM, Gottlieb GL, Agarwal GC (1989) Organizing principles for single joint movements. II. A speed-sensitive strategy. J Neurophysiol 62:358–368

Corcos DM, Gottlieb GL, Latash ML, Almeida GL, Agarwal GC (1992) Electromechanical delay: an experimental artifact. J Electromyogr Kinesiol 2:59–68

Crenna P, Frigo C (1991) A motor programme for the initiation of forward-oriented movements in humans. J Physiologie 437:635–653

Criswell E, Cram JR (2011) Cram's Introduction to Surface Electromyography. Jones and Bartlett, Sudbury

Cuadra C, Bartsch A, Tiemann P, Reschechtko S, Latash ML (2018) Multi-finger synergies and the muscular apparatus of the hand. Exp Brain Res 236:1383–1393

d'Avella A, Bizzi E (2005) Shared and specific muscle synergies in natural motor behaviors. Proc Nat Acad Sci USA 102:3076–3081
d'Avella A, Saltiel P, Bizzi E (2003) Combinations of muscle synergies in the construction of a natural motor behavior. Nat Neurosci 6:300–308
Danna-Dos-Santos A, Slomka K, Zatsiorsky VM, Latash ML (2007) Muscle modes and synergies during voluntary body sway. Exp Brain Res 179:533–550
Danna-Dos-Santos A, Degani AM, Latash ML (2008) Flexible muscle modes and synergies in challenging whole-body tasks. Exp Brain Res 189:171–187
De Freitas PB, Freitas SMSF, Lewis MM, Huang X, Latash ML (2018) Stability of steady hand force production explored across spaces and methods of analysis. Exp Brain Res 236:1545–1562
Diedrichsen J, Shadmehr R, Ivry RB (2010) The coordination of movement: optimal feedback control and beyond. Trends Cogn Sci 14:31–39
Duarte M, Freitas SMSF (2005) Speed-accuracy trade-off in voluntary postural movements. Mot Control 9:180–196
Falaki A, Huang X, Lewis MM, Latash ML (2016) Impaired synergic control of posture in Parkinson's patients without postural instability. Gait Posture 44:209–216
Falaki A, Huang X, Lewis MM, Latash ML (2017) Motor equivalence and structure of variance: Multi-muscle postural synergies in Parkinson's disease. Exp Brain Res 235:2243–2258
Falaki A, Jo HJ, Lewis MM, O'Connell B, De Jesus S, McInerney J, Huang X, Latash ML (2018) Systemic effects of deep brain stimulation on synergic control in Parkinson's disease. Clin Neurophysiol 129:1320–1332
Feldman AG (1966) Functional tuning of the nervous system with control of movement or maintenance of a steady posture. II. Controllable parameters of the muscle. Biophysics 11:565–578
Feldman AG (1986) Once more on the equilibrium-point hypothesis (λ-model) for motor control. J Mot Behav 18:17–54
Feldman AG (2015) Referent control of action and perception: Challenging conventional theories in behavioral science. Springer, New York
Freitas SMSF, de Freitas PB, Lewis MM, Huang X, Latash ML (2019) Quantitative analysis of multi-element synergies stabilizing performance: Comparison of three methods with respect to their use in clinical studies. Exp Brain Res 237:453–465
Frysinger RC, Bourbonnais D, Kalaska JF, Smith AM (1984) Cerebellar cortical activity during antagonist cocontraction and reciprocal inhibition of forearm muscles. J Neurophysiol 51:32–49
Gottlieb GL, Corcos DM, Agarwal GC (1989) Strategies for the control of voluntary movements with one mechanical degree of freedom. Behav Brain Sci 12:189–250
Hafström A, Modig F, Magnusson M, Fransson PA (2014) Effectuation of adaptive stability and postural alignment strategies are decreased by alcohol intoxication. Hum Mov Sci 35:30–49
Hair JF, Anderson RE, Tatham RL, Black WC (1995) Factor analysis. In: Borkowski D (ed) Multivariate data analysis. Prentice Hall, Englewood Cliffs, pp 364–404
Harris CM, Wolpert DM (1998) Signal-dependent noise determines motor planning. Nature 394:780–784
Hirokawa S, Solomonow M, Luo Z, Lu Y, D'Ambrosia R (1991) Muscular co-contraction and control of knee stability. J Electromyogr Kinesiol 1:199–208
Hogan N, Sternad D (2007) On rhythmic and discrete movements: reflections, definitions and implications for motor control. Exp Brain Res 181:13–30
Ivanenko YP, Poppele RE, Lacquaniti F (2004) Five basic muscle activation patterns account for muscle activity during human locomotion. J Physiol 556:267–282
Kaiser HF (1960) The application of electronic computers to factor analysis. Educ Psychol Meas 20:141–151
Kargo WJ, Ramakrishnan A, Hart CB, Rome LC, Giszter SF (2010) A simple experimentally based model using proprioceptive regulation of motor primitives captures adjusted trajectory formation in spinal frogs. J Neurophysiol 103:573–590
Kawato M (1999) Internal models for motor control and trajectory planning. Curr Opin Neurobiol 9:718–727
Klous M, Mikulic P, Latash ML (2011) Two aspects of feed-forward postural control: anticipatory postural adjustments and anticipatory synergy adjustments. J Neurophysiol 105:2275–2288
Krishnamoorthy V, Goodman SR, Latash ML, Zatsiorsky VM (2003a) Muscle synergies during shifts of the center of pressure by standing persons: Identification of muscle modes. Biol Cybern 89:152–161
Krishnamoorthy V, Latash ML, Scholz JP, Zatsiorsky VM (2003b) Muscle synergies during shifts of the center of pressure by standing persons. Exp Brain Res 152:281–292
Krishnan V, Aruin AS, Latash ML (2011) Two stages and three components of postural preparation to action. Exp Brain Res 212:47–63
Krishnan V, Latash ML, Aruin AS (2012) Early and late components of feed-forward postural adjustments to predictable perturbations. Clin Neurophysiol 123:1016–1026
Latash ML (2008) Synergy. Oxford University Press, New York
Latash ML (2010) Motor synergies and the equilibrium-point hypothesis. Mot Control 14:294–322
Latash ML (2012) The bliss (not the problem) of motor abundance (not redundancy). Exp Brain Res 217:1–5
Latash ML (2016) Towards physics of neural processes and behavior. Neurosci Biobehav Rev 69:136–146
Latash ML (2017) Biological movement and laws of physics. Mot Control 21:327–344
Latash ML (2018) Muscle co-activation: definitions, mechanisms, and functions. J Neurophysiol 120:88–104
Latash ML, Gottlieb GL (1991) Reconstruction of elbow joint compliant characteristics during fast and slow voluntary movements. Neurosci 43:697–712
Latash ML, Huang X (2015) Neural control of movement stability: Lessons from studies of neurological patients. Neurosci 301:39–48
Latash ML, Scholz JP, Schöner G (2002) Motor control strategies revealed in the structure of motor variability. Exer Sport Sci Rev 30:26–31
Latash ML, Scholz JP, Schöner G (2007) Toward a new theory of motor synergies. Mot Control 11:276–308
Leone FC, Nottingham RB, Nelson LS (1961) The folded normal distribution. Technometrics 3:543–550
Massion J (1992) Movement, posture and equilibrium—interaction and coordination. Progs Neurobiol 38:35–56
Mattos D, Latash ML, Park E, Kuhl J, Scholz JP (2011) Unpredictable elbow joint perturbation during reaching results in multijoint motor equivalence. J Neurophysiol 106:1424–1436
Mattos D, Kuhl J, Scholz JP, Latash ML (2013) Motor equivalence (ME) during reaching: Is ME observable at the muscle level? Mot Control 17:145–175
Milner TE, Cloutier C (1993) Compensation for mechanically unstable loading in voluntary wrist movement. Exp Brain Res 94:522–532
Mullick AA, Turpin NA, Hsu SC, Subramanian SK, Feldman AG, Levin MF (2018) Referent control of the orientation of posture and movement in the gravitational field. Exp Brain Res 236:381–398
Nielsen JB, Kagamihara Y (1992) The regulation of disynaptic reciprocal Ia inhibition during co-contraction of antagonistic muscles in man. J Physiol 456:373–391
Olafsdottir H, Yoshida N, Zatsiorsky VM, Latash ML (2005) Anticipatory covariation of finger forces during self-paced and reaction time force production. Neurosci Letts 381:92–96

Olafsdottir H, Yoshida N, Zatsiorsky VM, Latash ML (2007) Elderly show decreased adjustments of motor synergies in preparation to action. Clin Biomech 22:44–51

Park J, Lewis MM, Huang X, Latash ML (2014) Dopaminergic modulation of motor coordination in Parkinson's disease. Parkinsonism Rel Disord 20:64–68

Piscitelli D, Falaki A, Solnik S, Latash ML (2017) Anticipatory postural adjustments and anticipatory synergy adjustments: preparing to a postural perturbation with predictable and unpredictable direction. Exp Brain Res 235:713–730

Polit A, Bizzi E (1978) Processes controlling arm movements in monkey. Science 201:1235–1237

Rand MK, Van Gemmert AW, Hossain AB, Shimansky YP, Stelmach GE (2012) Control of aperture closure initiation during trunk-assisted reach-to-grasp movements. Exp Brain Res 219:293–304

Robert T, Zatsiorsky VM, Latash ML (2008) Multi-muscle synergies in an unusual postural task: quick shear force production. Exp Brain Res 187:237–253

Scholz JP, Schöner G (1999) The uncontrolled manifold concept: Identifying control variables for a functional task. Exp Brain Res 126:289–306

Scholz JP, Schöner G, Hsu WL, Jeka JJ, Horak F, Martin V (2007) Motor equivalent control of the center of mass in response to support surface perturbations. Exp Brain Res 180:163–179

Shadmehr R, Wise SP (2005) The computational neurobiology of reaching and pointing. MIT Press, Cambridge

Shim JK, Olafsdottir H, Zatsiorsky VM, Latash ML (2005) The emergence and disappearance of multi-digit synergies during force production tasks. Exp Brain Res 164:260–270

Slijper H, Latash ML (2000) The effects of instability and additional hand support on anticipatory postural adjustments in leg, trunk, and arm muscles during standing. Exp Brain Res 135:81–93

Slijper HP, Latash ML (2004) The effects of muscle vibration on anticipatory postural adjustments. Brain Res 1015:57–72

Tillman M, Ambike S (2018) Cue-induced changes in the stability of finger force-production tasks revealed by the uncontrolled manifold analysis. J Neurophysiol 119:21–32

Ting LH, Macpherson JM (2005) A limited set of muscle synergies for force control during a postural task. J Neurophysiol 93:609–613

Todorov E (2004) Optimality principles in sensorimotor control. Nat Neurosci 7:907–915

Venkadesan M, Guckenheimer J, Valero-Cuevas FJ (2007) Manipulating the edge of instability. J Biomech 40:1653–1661

Wang Y, Zatsiorsky VM, Latash ML (2005) Muscle synergies involved in shifting center of pressure during making a first step. Exp Brain Res 167:196–210

Wang Y, Asaka T, Zatsiorsky VM, Latash ML (2006) Muscle synergies during voluntary body sway: Combining across-trials and within-a-trial analyses. Exp Brain Res 174:679–693

Winter DA, Prince F, Frank JS, Powell C, Zabjek KF (1996) Unified theory regarding A/P and M/L balance in quiet stance. J Neurophysiol 75:2334–2343

Wolpert DM, Miall RC, Kawato M (1998) Internal models in the cerebellum. Trends Cogn Sci 2:338–347

Yamagata M, Falaki A, Latash ML (2018) Effects of voluntary agonist-antagonist co-activation on stability of vertical posture. Mot Control. https://doi.org/10.1123/mc.2018-0038

Zatsiorsky VM, Prilutsky BI (2012) Biomechanics of Skeletal Muscles. Human Kinetics, Urbana